

The Role of Operational Constraints in Selecting Supplementary Observations

JAMES A. HANSEN

*Space Science and Technology Department, Rutherford Appleton Laboratory, Chilton, Didcot, United Kingdom and
Department of Mathematics, University of Oxford, Oxford, United Kingdom*

LEONARD A. SMITH

Department of Mathematics, University of Oxford, Oxford, United Kingdom

(Manuscript received 12 November 1998, in final form 12 October 1999)

ABSTRACT

Adaptive observation strategies in numerical weather prediction aim to improve forecasts by exploiting additional observations at locations that are themselves optimized with respect to the current state of the atmosphere. The role played by an inexact estimate of the current state of the atmosphere (i.e., error in the “analysis”) in restricting adaptive observation strategies is investigated; necessary conditions valid across a broad class of modeling strategies are identified for strategies based on linearized model dynamics to be productive. It is demonstrated that the assimilation scheme, or more precisely, the magnitude of the analysis error is crucial in limiting the applicability of dynamically based strategies. In short, strategies based on linearized dynamics require that analysis error is sufficiently small so that the model linearization about the analysis is relevant to linearized dynamics of the full system about the true system state. Inasmuch as the analysis error depends on the assimilation scheme, the level of observational error, the spatial distribution of observations, and model imperfection, so too will the preferred adaptive observation strategy. For analysis errors of sufficiently small magnitude, dynamically based selection schemes will outperform those based only upon uncertainty estimates; it is in this limit that singular vector-based adaptive observation strategies will be productive. A test to evaluate the relevance of this limit is demonstrated.

1. Introduction

Just as the predictability of the atmosphere changes from day to day, so does the location at which an additional observation would most improve the forecasts of the day. The use of supplementary observations in numerical weather prediction (NWP) was first suggested by Emanuel et al. (1995), and has recently been considered by a number of authors [Langland and Rohaly (1996); Joly et al. (1997); Hansen (1998); Lorenz and Emanuel (1998); Palmer et al. (1998); Berliner et al. (1999); Bishop and Toth (1999); Joly et al. (1999, manuscript submitted to *Quart. J. Roy. Meteor. Soc.*)] who contrast a range of *adaptive observation strategies* (AOS) each attempting to determine the best location to observe. In general, the accuracy of forecasts for spatially extended nonlinear systems will vary with the quality of the model(s) employed, the uncertainty in the best estimate of the initial condition (hereafter, the anal-

ysis), and both the spatial distribution of and noise level in the observations. These basic issues are independent of the details of the physical system one is attempting to predict, suggesting that a general dynamical systems approach might provide insight for any operational application. Just such an approach was taken by Lorenz and Emanuel (1998, hereafter LE98), employing the 40-dimensional model introduced by Lorenz (1995). Drawing on results from Hansen (1998), we take a similar approach in the current paper, first demonstrating the explicit dependence of adaptive observation strategies on the data assimilation scheme employed. Second, we show that taking future dynamical information into account is beneficial, in contrast with the conclusions in LE98. General arguments suggest that AOSs based on singular vectors (see Palmer et al. 1998) will outperform other methods in certain limiting cases. Third, tests of internal consistency (Gilmour and Smith 1997; Gilmour 1998) are adopted to determine the relevance of the linear approximation crucial to the success of singular vector methods. The results of LE98 are explained in this context. The arguments of this paper also apply to cases of structural (as opposed to parametric) model error and the impact of structural error on adaptive ob-

Corresponding author address: Dr. James A. Hansen, Department of Earth, Atmospheric, and Planetary Sciences, Massachusetts Institute of Technology, 77 Massachusetts Avenue, Cambridge, MA 02139.
E-mail: jhansen@mit.edu

ervation strategies is documented using a distinct system, also introduced by Lorenz (1995).

Ideally, an adaptive observation strategy identifies the most valuable location at which an additional observation could be made. We demonstrate that, like forecast accuracy, the AOS that proves optimal also depends on the combination of model, assimilation scheme, and observational network; employing more complex AOSs that include model dynamics can be profitable when the analysis (and model) is accurate. The primary system, model, data assimilation schemes, and AOSs employed in this work are briefly introduced in section 2. The experimental design of LE98 is adopted in section 2 to allow for direct comparisons with previous work. In particular, the ranking of AOSs is shown to vary with changes in the assimilation scheme, even under the observational constraints used in LE98.

Fairly general conditions are identified within which the AOSs based on singular vectors are near optimal. In addition, necessary conditions for the relevance of singular vectors are derived in section 3, which clarify the reasons behind the poor results of LE98's singular vector AOS implementation. The importance of quantifying the relevance of the linearization assumption is stressed throughout, and a simple statistic for doing so is discussed. The importance of using a sensible metric in singular vector construction is then motivated, and the impact of analysis error magnitude on dynamically based AOSs is shown in section 4. Different assimilation schemes produce different levels of analysis error, and the rank ordering of the dynamically based AOSs is dependent on these analysis error levels. Our results generalize to the case of structural model error; section 5 introduces a different system and demonstrates the impact of structural model error on data assimilation schemes and adaptive observation strategies. A general discussion of the relevance of results given other observational constraints (like the chosen method for assessment) is given in section 6 where issues such as the spatial distribution of fixed observing systems are also touched upon. Section 7 provides a brief statement of conclusions and notes implications for operational forecasting.

2. Adaptive observation strategies

Lorenz (1995) introduced a 40-dimensional system that may be interpreted as representing an atmospheric quantity distributed zonally about the earth (see also Lorenz and Emanuel 1998; Hansen 1998). The equations are

$$\frac{dx_i}{dt} = -x_{i-2}x_{i-1} + x_{i-1}x_{i+1} - x_i + F, \quad (1)$$

$$i = 1, m,$$

where $m = 40$ and $F = 8$. The system is atmosphere-like in that it contains analogs to the basic atmospheric

physics of external forcing, internal dissipation, and convection. The boundary conditions are cyclic, and information propagates from low-indexed components to high-indexed components.¹ The system has been tuned to give characteristic length and timescales that are similar to the atmospheric system. For a more detailed discussion see LE98.

AOSs are contrasted using a structurally perfect forecast model of this system, allowing direct comparison with the results of LE98. Equations (1) are thus adopted as the forecast model for this system, the only model error being in the specification of the forcing, $F_{\text{model}} = 0.95F$. In practice, structural model error may well play a central role in an AOS, a point we return to in section 5. An observation consists of one component of the true state variable, x_i , plus one realization of an independent, normally distributed random variable with standard deviation σ_{obs} . Each component of \mathbf{x} is designated as either "land" or "ocean"; in the absence of an AOS, observations are made over land ($x_i, i = 21, \dots, 40$) every 6 model hours and no observations are made over the ocean ($x_i, i = 1, \dots, 20$). Thus the AOS will select one of the 20 distinct components at which an additional observation can be made.

Where should additional observations be made? In this paper, the "best" observation is defined as that which results in the smallest distance between the forecast state and the true state at a chosen verification time, τ_{ver} , taken here to be 3 days. The AOS that results provides an upper bound against which all other AOSs can be gauged. This strategy is called the "forecast error" AOS (FEAOS) (see Table 1 for a summary of the AOSs considered in this work). This best location need not correspond either to the component that is most in error (the basis for the "analysis error" AOS, hereafter AEAOS), or to the location that would yield the greatest decrease in the analysis error;² in an imperfect model scenario, the smallest forecast error need not result from perfect initial conditions, and even when a perfect model is in hand, state-dependent uncertainty dynamics suggest that the smallest (finite) analysis error need not result in the smallest forecast error. Of course, none of these three strategies can be implemented operationally, as each requires knowledge of the true state of the system, but they do provide a benchmark against which operationally obtainable selection strategies can be assessed.

When the true state is not known, selection can target the component with the largest *estimated* analysis error, or uncertainty, (hereafter AUAOS). There are many ways to estimate the uncertainty associated with a given

¹ The term *component* is used throughout this work to denote individual x_i 's.

² This AOS is identical to the AEAOS for replacement assimilation (discussed below), but is heavily dependent on the data assimilation scheme employed for more complex data assimilation schemes.

TABLE 1. Adaptive observation strategy acronyms, names, descriptions, and whether or not they are operationally realizable.

Acronym	Name	Description	Realizable?
ROS	Random	Ocean components are selected at random	Yes
FEAOS	Forecast error	Ocean component that results in smallest three-day zonally averaged prediction error is selected	No
AEAOS	Analysis error	Ocean component with the largest analysis error is selected	No
AUAOS	Analysis uncertainty	Ocean component with the largest <i>expected</i> analysis error (estimated analysis error variance) is selected	Yes
MBAOS	Multiple breeding	Ocean component selected to minimize projection of resulting analysis error into the direction of large expected error growth given by bred vectors	Yes
SVAOS	Singular vector	Ocean component selected to minimize projection of resulting analysis error into the direction of large expected error growth given by singular vectors	Yes

analysis. A “multiple replication” method was employed by LE98, but the current paper also considers uncertainty estimates provided directly by the data assimilation scheme. Both the particular component with the largest estimated analysis error and the analysis uncertainty itself, will, of course, depend on the assimilation scheme employed. A primary goal of this paper is to demonstrate the central role the assimilation scheme plays in determining the optimal AOS in a given scenario. Two schemes are used to reflect the range of possible sequential assimilation implementations: replacement and the Kalman filter. Under assimilation by replacement (Lorenz and Emanuel 1998), the value of each observed component is adopted directly into the model state. Alternatively, the ensemble Kalman filter (hereafter EnKF) (Evensen 1994; Evensen and van Leeuwen 1996) melds model forecasts with observations by weighting each source of information according to its associated uncertainty. These two schemes were chosen to contrast the cases of large analysis error (replacement) and small analysis error (EnKF). To insure an accurate analysis in the latter case, a large ensemble ($N_{\text{ens}} = 1024$) was used in the EnKF. Utilising the EnKF as an assimilation scheme naturally suggests employing ensemble forecasts, an approach that will be pursued in future work.

Selecting ocean locations at random (the ROS) and assimilating them using replacement provides a minimal standard that a more complicated AOS must surpass.³ Forecast error of this baseline AOS is contrasted with forecast error with no AOS (i.e., no ocean observations) in Figs. 1a,b, which mirror Figs. 5 and 6 of LE98. Note that in contrast to LE98, time increases upward in the figures of the current paper. The ROS results of Fig. 1b are clearly superior, in particular the noticeable improvement about the central land–ocean boundary near x_{20} where the rms error does not reach a value of 4 until day 3 in the ROS case. Contrasting Figs. 1c and 1b

reveals the importance of the assimilation scheme given the same AOS; Fig. 1c shows the result of employing EnKF assimilation and random selection. Figure 1d is discussed in section 6.

LE98 evaluated two strategies based on model dynamics: the multiple breeding AOS (MBAOS) and the singular vector AOS (SVAOS). The MBAOS presented here is a replication of their scheme and can be interpreted as a dynamically based method for estimating analysis uncertainty. A common interpretation of bred vectors is that they consist of a linear combination of only the most rapidly growing directions of the recent past (see Toth and Kalnay 1993). Insofar as errors in an analysis will have experienced growth similar to that of the bred vectors members, it is argued that large discrepancies between an analysis and bred vector members corresponds to large expected analysis error. In contrast, the SVAOS aims to combine estimates of analysis uncertainty with future error growth to estimate directions in which perturbations will result in the largest expected forecast errors. The SVAOS implemented in this paper differs in choice of optimization time and norm from that of LE98 (see section 3). Lorenz and Emanuel conclude that the SVAOS proved “unproductive” for $\sigma_{\text{obs}} = 0.2$ and replacement assimilation. This conclusion is supported in Fig. 2b, which indicates that, in this case, SVAOS is worse than both the MBAOS (Fig. 2a) and the ROS (Fig. 1b). LE98 argue that the magnitude of forecast errors would change for different assimilation schemes, but the relative scoring positions of various AOSs would, most likely, remain the same. This is not the case, as we show in section 4. The relevance (or lack thereof) of the singular vectors upon which the SVAOS is constructed is dependent upon the relevance of the associated (model) linear propagator. In the next section, the assumptions that underly *any* application of the linear propagator to an AOS are clarified and a test of its relevance is given. Whenever the linear propagator is rendered irrelevant, the SVAOS must prove unproductive. Changing operational constraints (in particular, reducing the analysis error) will alter the rank order of AOS performance.

³ A reviewer suggested alternative baselines. While a variety of options are contrasted in Hansen (1998), random selection was deemed to be the most illustrative.

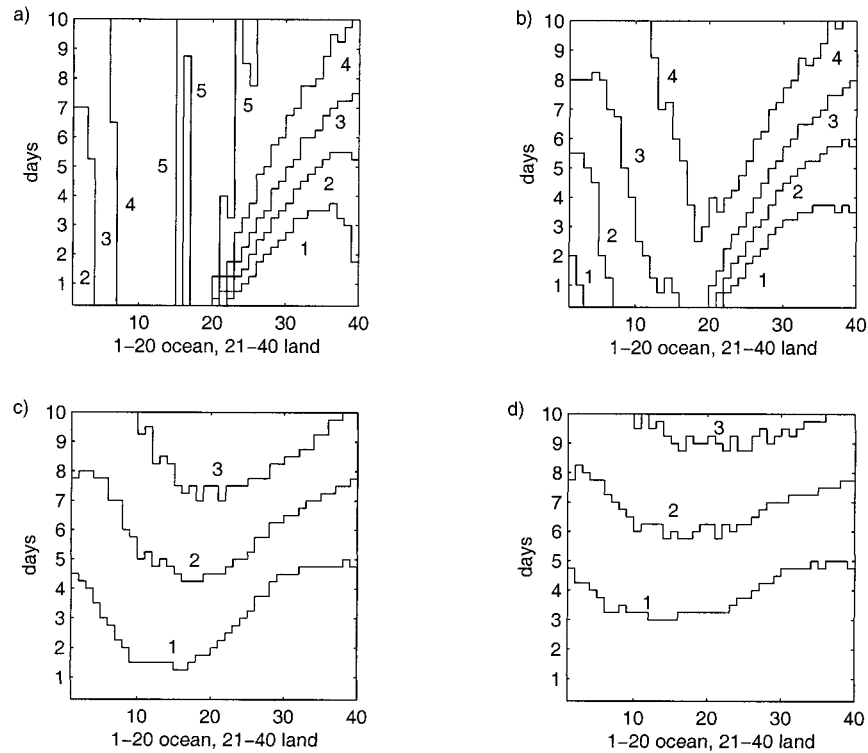


FIG. 1. Contours of rms prediction error for different combinations of AOS and assimilation scheme. (a) No selection using replacement, (b) ROS using replacement, (c) ROS using the EnKF, (d) ROS using the EnKF with an observational backbone that includes two islands and two lakes (discussed in section 6). The model components are spaced across the x axis, with components 1–20 over ocean and 21–40 over land. Prediction time increases along the y axis.

3. On the relevance of linearized dynamics

Methods based on linearizations will only be effective when the linearized dynamics of the model match the linearized dynamics of the underlying system. While this fact is widely acknowledged (Vukićević 1991; Palmer et al. 1994; Buizza and Palmer 1995), consistency is seldom tested for explicitly (exceptions include Errico et al. 1993; Buizza 1995; Gilmour and Smith 1997; Gilmour 1998). The relevance of a linearity assumption will, of course, depend on the quality of the model, but also on the quality of the analysis and on the verification time. Even given a perfect model, the relevance of each linearization will vary with the state of the system (it is time dependent), the size of the initial error and the timescale over which the linearization is carried out. For a perfect model and infinitesimal errors, the linearization approximation holds for all time; finite initial errors almost certainly imply its failure at finite time. To demonstrate the linearization assumption validity's dual dependence on verification time and initial error magnitude, consider an initial condition of a nonlinear, deterministic system, and imagine isotropic uncertainty isopleths of increasing magnitude associated with that initial condition. If the initial condition and associated uncertainty isopleths are evolved forward un-

der the full nonlinear flow, the initially isotropic uncertainty isopleths will, after a short time, evolve into hyper-ellipses, as would be specified by a linear uncertainty propagator. At longer times, one expects a breakdown of the linear approximation first for the isopleths corresponding to the largest initial uncertainty magnitude, but eventually for *all* isopleths of initially finite magnitude. For *any* optimization time there exists an initial uncertainty magnitude beyond which the linearization assumption fails.

The Θ statistic was introduced in order to ascertain whether or not techniques based on the linear propagator might be productive in operational NWP forecasts (Smith and Gilmour 1998; Gilmour 1998). This statistic is defined by examining the evolution of twin perturbations about a control trajectory. Given a model state, $\mathbf{x}(t_0)$, the twin perturbations are defined by adding and subtracting the same (vector) perturbation δ to $\mathbf{x}(t_0)$. Thus in addition to the fiducial trajectory from $\mathbf{x}(t_0)$, two additional trajectories are defined as $\mathbf{x}^+(t_0) = \mathbf{x}(t_0) + \delta^+(t_0)$ and $\mathbf{x}^-(t_0) = \mathbf{x}(t_0) + \delta^-(t_0)$, where $\delta^+(t_0) = -\delta^-(t_0)$. The final time perturbations at $t = t_0 + \tau$ are then $\delta^+(t) = \mathbf{F}_t[\mathbf{x}^+(t_0)] - \mathbf{F}_t[\mathbf{x}(t_0)]$ and $\delta^-(t) = \mathbf{F}_t[\mathbf{x}^-(t_0)] - \mathbf{F}_t[\mathbf{x}(t_0)]$ where $\mathbf{F}_t(\mathbf{x})$ indicates the image of an initial condition \mathbf{x} evolved under model \mathbf{F} for time

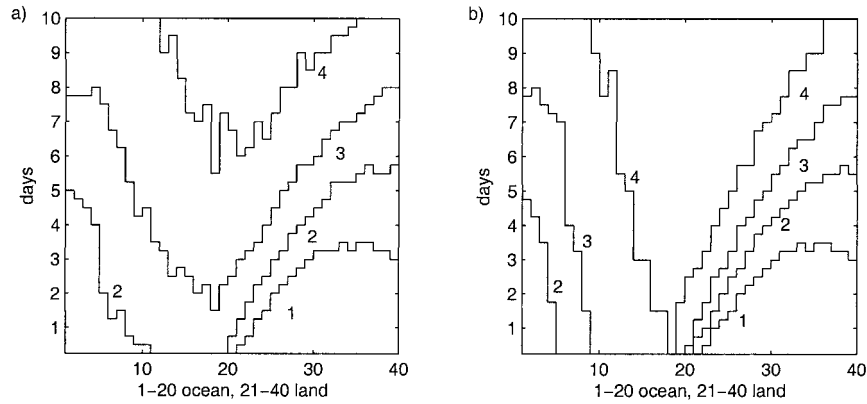


FIG. 2. Contours of rms prediction error for (a) the MBAOS using replacement, and (b) the SVAOS using replacement. Note that the SVAOS under replacement is inferior to the ROS (shown in Fig. 1b.)

t . The degree to which $\delta^+(t)$ approximates $-\delta^-(t)$ reflects the degree to which the linear approximation of F holds at time t . This can be quantified as

$$\Theta(t_0, \delta(t_0), t) = \frac{\|-\delta^+(t) + \delta^-(t)\|}{\frac{1}{2}(\|\delta^+(t)\| + \|\delta^-(t)\|)} \quad (2)$$

as illustrated in Fig. 3.

When the linear approximation is exact, $\Theta = 0$ for all initial orientations, while when $\Theta = 1$ the error associated with the linear approximation are equal in magnitude to the evolved perturbations themselves. By construction $\Theta \leq 2$, with $\Theta = 2$ indicating that the vectors are oriented in the same direction; that is $\|\delta^+(t)\| = \|\delta^-(t)\|$. For the 40-dimensional model considered here, Θ saturates to a value of $\Theta = 1.73$ for large verification times and/or large initial perturbation magnitudes. Note that $\Theta = 0$ is a necessary, but not sufficient condition for assessing linearity assumption validity.

The Θ statistic will vary with (i) initial condition, (ii) initial perturbation direction, (iii) initial perturbation magnitude, and (iv) verification time. A general picture of “the linear range” may be obtained by tracing contours of the median value of Θ as a function of both verification time and the magnitude of the initial uncertainty, where the median is evaluated over many initial conditions. Figures 4a,b show these contours for

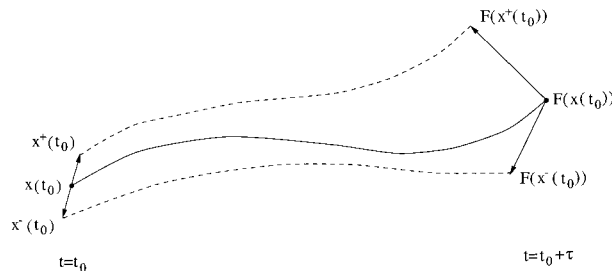


FIG. 3. Construction of the Θ statistic. See text for details.

randomly oriented initial perturbations and Figs. 4c,d for initial perturbations oriented in a locally most unstable direction defined by singular vectors optimized over two model days.

The reason why Lorenz and Emanuel found the singular vector AOS to be unproductive is revealed by Fig. 4: a 10 day optimization time results in an expected analysis uncertainty magnitude of 4.13 [using multiple replication, see Lorenz and Emanuel (1998) for details]. Figure 4 suggests that the error in the linear approximation for such a magnitude is well over 100% even for randomly oriented initial perturbations (note that such an error value is beyond the range of the plot). In this case even the system’s exact linear propagator has little relevance to the dynamics of the analysis; if, however, the analysis error and/or optimization time can be reduced then this need not remain the case, as illustrated in section 4 below. First, the current paper’s implementation of the singular vector AOS is specified.

The singular value decomposition (SVD) of a model linear propagator requires a choice of metric on the model state space. For the cases considered here, this metric is specified by a matrix defining the unit of distance in each state space direction. The implicit metric (the identity matrix) chosen by LE98 implies isotropy. For an SVD in the AOS context the metric should reflect uncertainty in the analysis that is *never* isotropic in these land–ocean experiments. Failure to account for this lack of isotropy can result in irrelevant singular vectors, even when the linear approximation is relevant. For this reason, we adopt a metric specified by the inverse of the (local) analysis error covariance matrix. Schematically, such a metric is easily motivated; the forecast error resulting from a relatively small growth of an initially huge uncertainty may easily dominate the relatively large growth of an initially tiny uncertainty. Detailed algebraic arguments (and references) are given in the appendix. The important quantity is the forecast error at final time, which depends on the combination of ef-

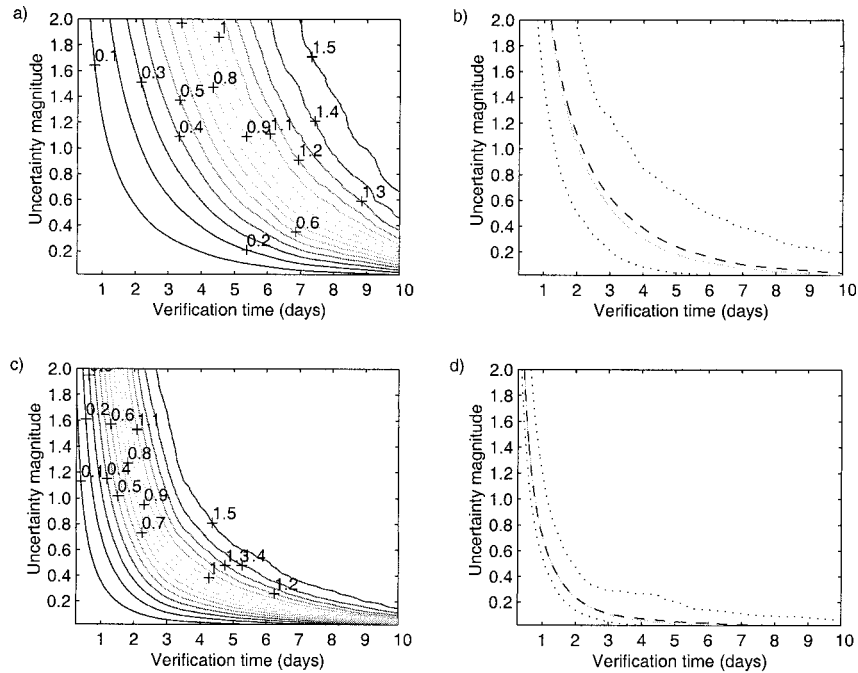


FIG. 4. Contours of Θ as a function of verification time (x axis) and magnitude of initial perturbation (y axis). Contours of Θ measures the degree to which a system is behaving non-linearly; $\Theta = 0$ is a necessary, but not sufficient condition for uncertainty growth behaving perfectly linearly. For $\Theta = 1$, the errors associated with the linear assumption are of the same magnitude as the final perturbations. (a) Shows contours of median Θ for initial perturbations oriented in random directions. (b) For the same situation as (a), but showing only the mean (solid), median (dashes), and 1st and 99th percentiles (dotted) of the $\Theta = 0.2$ contour. (c) and (d) Are identical to panels (a) and (b), respectively, but for perturbations oriented in the direction of the first singular vector optimized over two model days. In all cases, 512 different initial conditions are considered.

fective growth factors and initial amplitudes. Exploiting this metric operationally requires an estimate of the analysis error covariance matrix. There are a number of methods to provide such estimates, including both static estimates (independent of system state) and dynamic estimates (usually) derived either from data assimilation schemes or from ensemble approaches (as in the case of LE98's multiple replication AOS). This paper also takes an ensemble approach, employing uncertainty estimates that are a by-product of the EnKF.

There is a close relationship between the uncertainty estimates produced by LE98's multiple replication and those produced by the EnKF. Both result from the independent assimilation of an ensemble of states, each with a different realization of observational noise. The primary difference between the two is that the independent assimilation of the EnKF is intrinsic to the data assimilation scheme, while for multiple replication it is separate from the data assimilation scheme. Implementing a multiple replication approach under the EnKF produces results similar to the EnKF-based AUAOS.

4. AOSs and analysis error

Reducing the analysis error holds significant implications for an operational AOS. These implications are

now quantified through comparison with the ideal FEAOS. This comparison shows that the SVAOS under EnKF assimilation may provide a viable strategy even for the observational conditions used by LE98. As observational error is reduced (thereby reducing the analysis error), the SVAOS performance is enhanced to the point where it outperforms first the MBAOS, and then the AUAOS. In general, as the analysis error approaches zero the SVAOS is expected to outperform *any* strategy based solely on analysis uncertainty information⁴ within perfect a model. This need not be the case for an imperfect model, which we return to in section 5. First, the impact of the particular data assimilation scheme employed is demonstrated in section 4a, and the impact of variations in the magnitude of expected observational error on the AOS performance is presented in section 4b.

a. Dependence on assimilation scheme

Given a component-wise observational uncertainty drawn from a Gaussian distribution with $\sigma_{\text{obs}} = \sigma_{\text{LE98}}$

⁴ Regardless of whether this is done by breeding, AUAOS, or some other method.

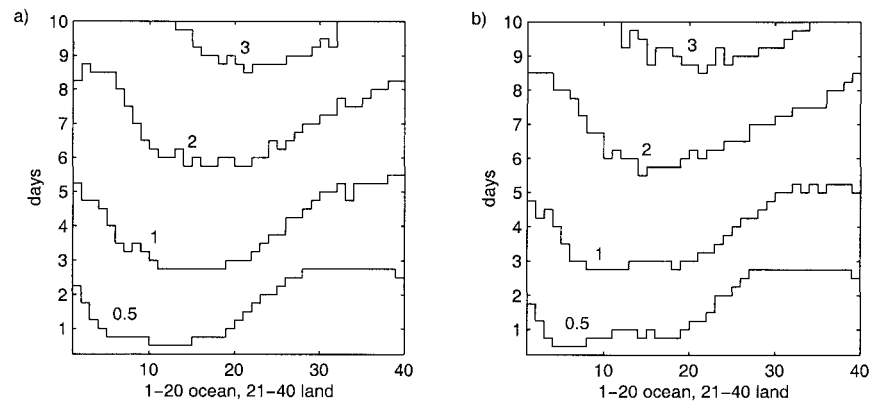


FIG. 5. Contours of rms prediction error under the EnKF assimilation scheme for (a) the MBAOS and (b) the SVAOS (with the analysis error covariance norm). Contrary to the replacement results of Fig. 2, the SVAOS is providing results comparable to the MBAOS.

$= 0.2$, a 6-h sampling time, and a 10-day optimization time (as specified in LE98), the performance of the SVAOS is poor under replacement assimilation⁵ (see Fig. 2b). Employing the EnKF assimilation scheme, however, changes the rank ordering of the AOSs. The SVAOS not only outperforms the ROS, but is comparable with, although slightly inferior to, the MBAOS when EnKF assimilation is applied. This result is quantified in Figs. 5a and 5b. The AUAOS, however, produces forecasts (not shown) that outperform both the SVAOS and MBAOS, suggesting that given these particular operational constraints more value is obtained from uncertainty information than from dynamical information.

The absolute quality of these selection schemes may be evaluated through comparison with the FEAOS, in which the location observed is that which yields the minimum three day, zonally averaged rms forecast error. While the FEAOS is, of course, not feasible operationally, its role here is to quantify how close the operational AOSs are to this ultimate target. Figure 6 contrasts the FEAOS in Fig. 6b with the AEAOS in Fig. 6a, both under EnKF assimilation; the results of AEAOS are, in general, inferior to the FEAOS. This inferiority is even more pronounced under replacement (not shown). Thus, Fig. 6 indicates that there is useful information in the future dynamics of the system; any AOS that is able to successfully capture this information will outperform an AOS based only on current or past information. The three-day verification time was chosen to be representative of “medium-range” forecasts, and it proved adequate for illustrating the importance of future dynamics. Comparing results from FEAOSs constructed over different lead times would prove informative for this particular system, but would serve only to strengthen the above result. The importance of an accurate line-

arization is amplified in the case of an imperfect model. In an imperfect model, the smallest analysis error, even if it is zero, need not result in the smallest forecast error. For the conditions of LE98, the average analysis error for the AEAOS is 1.14, while the average analysis error for the FEAOS is 1.67. On average, the AEAOS produces smaller forecast errors for lead times less than 1.5 model days, and the FEAOS produces smaller forecasts for longer lead times.

Contrasting the panels in Fig. 6 with those in Fig. 5 indicates that both the multibreeding AOS and singular vector AOS are productive; further, *both* are approaching the best performance possible.

b. Dependence on observational noise level

The analysis error will also be reduced if observational noise is decreased, again extending the range over which the linear approximation is relevant. When the component-wise observational uncertainty is reduced by a factor of 16 (i.e., $\sigma_{\text{obs}} = \sigma_{\text{LE98}}/16 = 0.0125$), the SVAOS (Fig. 7b) outperforms the MBAOS (Fig. 7a). This result becomes more obvious if one concentrates on a single forecast time. Figure 8 shows average three-day forecast errors over the ocean as a function of expected component-wise observational uncertainty for the AUAOS, SVAOS, and MBAOS for four different levels of observational uncertainties. Results from three independent experiments are shown. As σ_{obs} decreases, there are three changes in the rank ordering of the AOSs. For $\sigma_{\text{obs}} = \sigma_{\text{LE98}}$, the rank ordering is 1) AUAOS, 2) MBAOS, and 3) SVAOS. At $\sigma_{\text{obs}} = \sigma_{\text{LE98}}/4$, the ordering has changed so that the SVAOS and AUAOS give comparable results and both outperform the MBAOS. At $\sigma_{\text{obs}} \leq \sigma_{\text{LE98}}/16$, the rankings appear to have converged to 1) SVAOS, 2) AUAOS, and 3) MBAOS. Ultimately, the model error present in the LE98 configuration will limit the level to which the analysis error can be reduced, even given perfect observations. The results of these

⁵ Changing the metric does not appreciably alter the results.

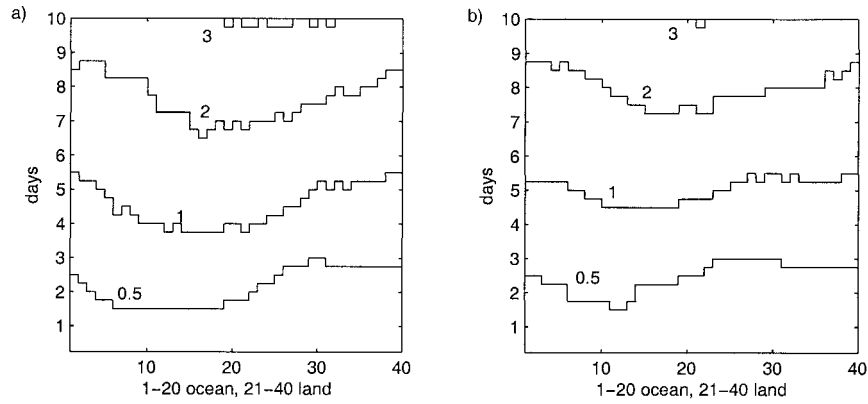


FIG. 6. Contours of rms prediction error for operationally infeasible, “perfect knowledge” AOSs. (a) the AEAOS using EnKF assimilation, and (b) the FEAOS (defined at three days) using EnKF assimilation. The fact that the FEAOS outperforms the AEAOS suggest that there is useful information contained in the future dynamics of the model.

operationally feasible AOSs are compared with those of the ideal AOS (the nonoperational FEAOS), shown as diamonds.

In general, as the observational uncertainty decreases so too will the analysis error, and an AOS based on model linearization will come to the fore. The Θ statistic provides a test of whether (or not) one can expect a linearization-based approach to provide relevant information. For LE98 conditions a linearization-based approach cannot; uncertainty rules. The Θ test is easily applied to operational models (as in Gilmour 1998), and once the Θ test is satisfied, techniques based on the linearity assumption become viable candidates. One must keep in mind that while the Θ statistic can inform when singular vectors are expected to be relevant, it need not imply that they are the best choice for the basis of an AOS. We agree with an anonymous referee that this test is rather obvious, and hope it will be widely implemented as it has already revealed shortcomings both in an operational AOS and in the common assumption that the linear range in numerical weather pre-

diction extends to 48 h (Smith and Gilmour 1998; Gilmour 1998).

5. AOSs and model error

Lorenz and Emanuel considered parametric model error; the difference between the system and model was only in the magnitude of the external forcing term [see Eq. (1)]. This section focuses on *structural* model error. A model that lacks essential dynamics will be used to assimilate and predict the behavior of a more complex system. The new system is constructed by coupling the ordinary differential equations (ODEs) of Eq. (1) (subsequently denoted Model I), with a second set of ODEs. This second set of ODEs has a characteristic timescale that is faster than that in Model I, and a spatial scale that is smaller than that in Model I. The coupling of these two sets of ODEs defines a system designated System II. Following Lorenz (1995), the system equations take the form

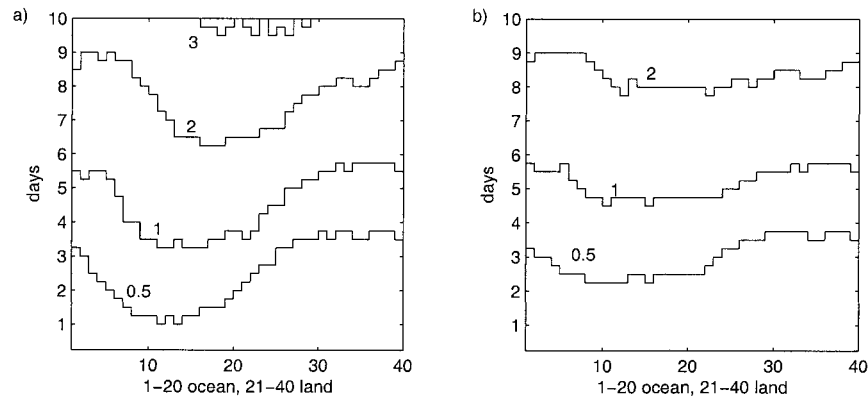


FIG. 7. Contours of rms prediction error for observational noise level at a 16th of that of Fig. 5. Panel (a) is the MBAOS result and panel (b) the SVAOS result. The decrease in observational error results in a decrease in analysis error, allowing the SVAOS to outperform the MBAOS.

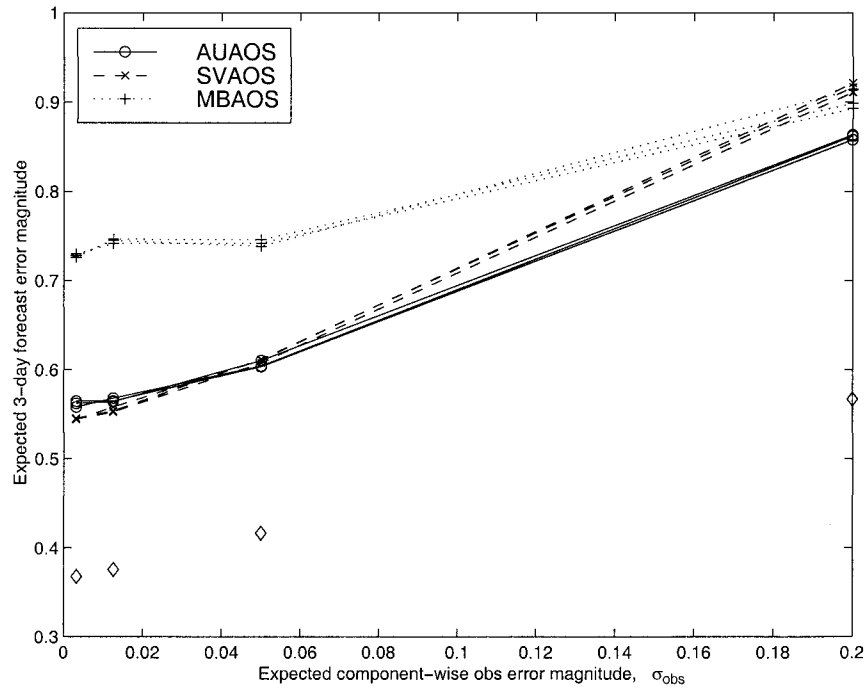


FIG. 8. Average three-day forecast errors over the ocean as a function of expected observational error magnitude (σ_{obs}) for the AUAOS, SVAOS, and MBAOS under EnKF assimilation. Results for σ_{LE98} , $\sigma_{\text{LE98}}/4$, $\sigma_{\text{LE98}}/16$, and $\sigma_{\text{LE98}}/64$ are shown. Results from three independent experiments are presented for each AOS to help quantify the variation in the results. As the component-wise expected observational error magnitude (σ_{obs}) is decreased, the SVAOS and AUAOS show marked improvement over the MBAOS. For the $\sigma_{\text{LE98}}/16$ and $\sigma_{\text{LE98}}/64$ cases, the SVAOS both outperforms the AUAOS and shows a stronger convergence of results. The combination of the spatial distribution of observations and the model error makes smaller analysis errors difficult to achieve, even with vanishingly small observational error. The diamonds reflect the smallest possible forecast error obtained by assimilating an observation from each ocean component in turn and selecting the one which yields the smallest three-day forecast error; this is the (nonoperational) FEAOS.

$$\frac{dx_i}{dt} = -x_{i-2}x_{i-1} + x_{i-1}x_{i+1} - x_i + F - \frac{h_x c}{b} \sum_{j=1}^J y_{j,i}, \quad (3)$$

$$\frac{dy_{j,i}}{dt} = -cby_{j+1,i}y_{j+2,i} + cby_{j-1,i}y_{j+1,i} - cy_{j,i} + \frac{h_x c}{b} x_i. \quad (4)$$

As is the case for the large-scale variables (x_i), the small-scale variables as a whole ($y_{j,i}$) have cyclic boundary conditions. Sectors of small-scale variables of size J are coupled to each of the large-scale variables. Each of the small-scale sectors are coupled by setting $y_{j-i,i} = y_{j,i-1}$ and $y_{j+J,i} = y_{j,i+1}$. Just as the x_i can be considered as some atmospheric quantity distributed zonally about the globe, so too can the $y_{j,i}$ with J small-scale variables associated with each of the large-scale variables. The constants c and b are both set to the value of 10; thus the small-scale dynamics operate on a scale 10 times as fast and 1/10th as large as the large-scale dynamics. The value of J , the number of small-scale variables coupled to each large scale, is set to 5. With x_i , $i = 1, 40$, the associated dimension of the $y_{j,i}$ s is 200, and System II has a 240-D state space. The values of h_x and h_y , the

coupling coefficients, are set to unity. For the experiments discussed below, $m = 40$ and $F = 8.0$.

Model I is used to assimilate observations drawn from the large-scale components of System II, and then predict the large-scale components' future evolution. It is necessary to parameterize the impact of Model I's missing dynamics. The combination of the external forcing term and the coupling term in Eq. (3) can be considered as an effective forcing term that varies deterministically in space and time. This effective forcing is parameterized to zeroth order by applying its mean value as a fixed forcing term in Model I.

Repeating the experiments of section 4 using the new model-system configuration yields the results of Fig. 9 that show that this level of model error strengthens the data assimilation scheme dependence of AOSs; the MBAOS results in Fig. 9a are markedly inferior to the SVAOS results in Fig. 9b. Even at this level of model error the EnKF is able to move the analysis close enough to the system state for the linearity approximation intrinsic to singular vectors to be of value.

The dependence of AOS on observation error mag-

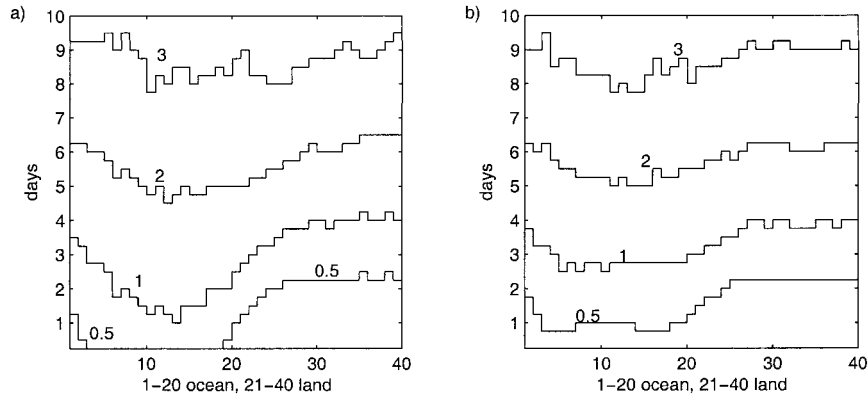


FIG. 9. Contours of rms prediction error under the EnKF assimilation scheme for (a) the MBAOS and (b) SVAOS (with the analysis error covariance norm) in the case where the model is structurally imperfect. The MBAOS is less robust than the SVAOS under this level of model error.

nitude is demonstrated in Fig. 10. Inasmuch as both the SVAOS and AUAOS significantly outperform the MBAOS at all observational error magnitudes considered, only values of ocean-averaged, three-day forecast errors for the SVAOS and AUAOS as a function of expected observational error magnitude are shown. Again four different expected observational uncertainties are considered, σ_{LE98} (beyond the range of the plot), $\sigma_{LE98}/4$, $\sigma_{LE98}/16$, and $\sigma_{LE98}/64$. Again results from three

independent experiments are shown. For $\sigma_{obs} \geq \sigma_{LE98}/64$, the SVAOS and AUAOS are comparable. It is only at $\sigma_{obs} = \sigma_{LE98}/64$ that there is a distinction between the two strategies with the SVAOS producing smaller forecast errors. The spread among the three realizations for each AOS is larger than for the parametric model error case (Fig. 8), suggesting that even after 5.5 model years, the results have not fully converged. The reason for this lack of convergence lies both in the AOS

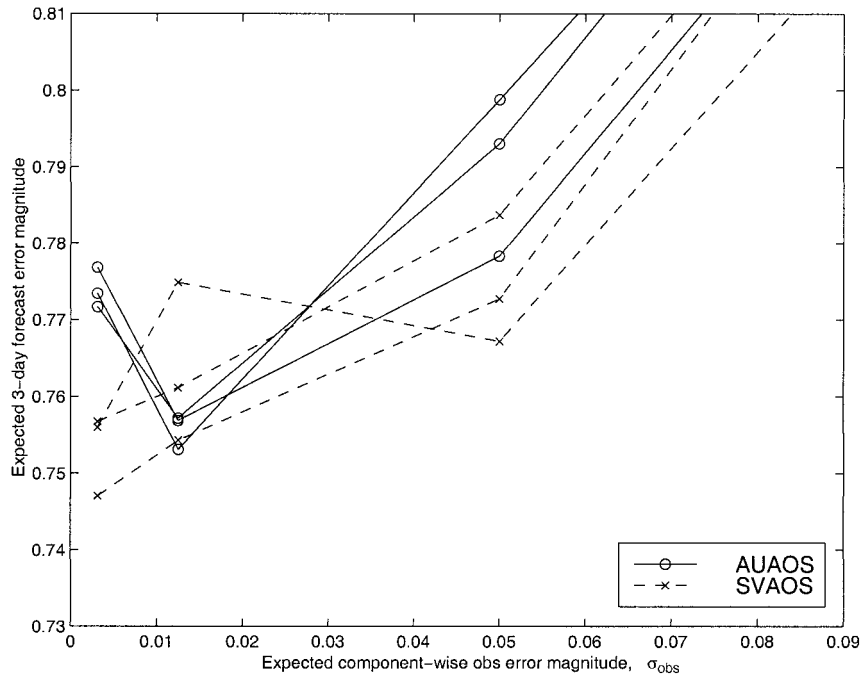


FIG. 10. Magnitude of the three-day forecast errors averaged over the ocean for the structurally imperfect model as a function of expected observational error magnitude (σ_{obs}) for the AUAOS, and SVAOS (the MBAOS is off the scale of the plot). Results for $\sigma_{LE98}/4$, $\sigma_{LE98}/16$, and $\sigma_{LE98}/64$ are shown. Results from three independent experiments are presented for each AOS to illustrate the variability in the results. For $\sigma_{obs} \leq \sigma_{LE98}/16$, the SVAOS and AUAOS produce comparable results. SVAOS outperform AUAOS for the smallest expected observational uncertainty level, $\sigma_{LE98}/64$.

and the data assimilation scheme. For this level of model error there is an increased autocorrelation in the analysis (and forecast) errors relative to the parametric model error case, reflecting the difficulty the AOS and data assimilation scheme have reestablishing an accurate analysis once a poor analysis has been generated.

There are, of course, many approaches to dealing with model error. In this section a classical physicists' model error has been discussed; model and system are deterministic systems, but different. An alternative approach (as in Berliner et al. 1999) is to include stochastic elements in the model. Both approaches are fundamentally flawed, since the true physical system is almost certainly not in either model class. Since we cannot account for realistic model error, we have instead developed algorithms that aim to quantify the effects and limitations imposed by particular types of model error in cases of interest. The aim is to attempt to explore the possible range of behavior; by construction, the results will depend on both the system and the model.

6. Discussion

In this work, the primary means of AOS assessment has been through global patterns of forecast error. This statistic was chosen to ease comparison with the work of LE98. It is important to note, however, that the rank ordering of AOSs may vary with the type of assessment statistic employed. Alternatives to the statistics used here include other characteristics of the distribution of prediction error constructed at a specified location in space and/or forecast time. For relatively simple systems, like Eq. (1) one may select each ocean location in turn, rank each location on the basis of a particular statistic, and then determine how well a particular AOS performs at selecting high-ranked locations. Employing this method of assessment shows that the SVAOS is adept at selecting high-ranking locations when the linearity assumption is good, and adept at selecting low-ranking locations when the linearity assumption is poor, or the choice of norm is poor. These, and other, alternative methods of evaluation are discussed by Hansen (1998).

The performance of an AOS also varies with the spatial structure of the observational network. Figure 1d shows the rms forecast error using the ROS when the observational "backbone" differs from that of 20 adjacent observations over land adopted for all other adaptive observation experiments in this work. In Fig. 1d, the observational backbone has been altered so that there are two "lakes" in the land components (components 27 and 34) and two "islands" in the ocean components (components 7 and 14). The lakes are never observed, and the islands are continuously observed. The ROS with this backbone systematically outperforms the ROS on the original distribution of land-ocean, even though 21 components are observed in each case. In general, given a perfect model and a particular backbone, a

smaller analysis error will imply better AOS results (assuming that the AOS is productive in the first place). Altering the backbone itself, however, alters the distribution of analyses in model state space in quite a different manner than merely reducing σ_{obs} . The impact this has on the relevance of the linear approximation will be heavily model dependent.

Ideally, a data assimilation scheme aims at the synchronization of model and system (see Pecora and Carroll 1990 and references thereof) given a noisy, one-way coupling. The difficulty of synchronizing model and system will depend not only on the strength and structure of the coupling, but also on the effects of structural model error, which may well dominate both. It is interesting to note that Eqs. (1) support strange, chaotic attractors that exist within proper subspaces of the full state space (these include system initial conditions of equations 1 with periodic symmetry in the index i); if the system evolves on such an attractor, it is not clear that the model will synchronize with the system even in the absence of model error (results to be reported elsewhere).

In the experiments presented in this paper, the system appeared to evolve in the full state space.⁶ Further, the forecast experiments were initialized from initial system states that sampled the range of variability exhibited by the system. In each case the initial analyses had been "spun up" with the aim of avoiding the effects of initial transients in the assimilation scheme.

7. Conclusions

The performance of several adaptive observation strategies and assimilation schemes have been contrasted in two simple, nonlinear systems. Variations in the preferred AOS are linked to the level of observational uncertainty, to the assimilation scheme, and to the level of model error; in particular, the SVAOS is shown to be productive in cases where the linear approximation assumed in its construction is relevant. Under EnKF assimilation, the SVAOS is shown to be comparable to other methods at the same noise level investigated by LE98, who concluded that the SVAOS was inferior (under replacement assimilation). Both sets of results are consistent and easily understood via explicit estimates of the relevance of the linear approximation. The method of estimating the limit of the linear range can (and should) be used whenever twin perturbations are evolved. Others (Berliner et al. 1999) have constructed a statistical framework for evaluating AOSs under the assumption that the linear approximation is relevant; we have attempted to quantify the relevance of the approximation.

⁶ An analysis of the structure of this (and the symmetric) chaotic attractor is given in Hansen (1998).

In the limit as the analysis error approaches zero, the system's future dynamics can always be utilised to determine where observations should be made in a perfect model, and the SVAOS is the preferred AOS. For larger analysis errors and/or imperfect models, the uncertainty in the analysis can swamp the information in the model's future dynamics, and the dynamically based AOSs need not outperform a strategy based purely on uncertainty estimates (the AUAOS). The statistical approach to the problem of AOS design taken by Berliner et al. (1999) considers white-noise model error. Our approach differs by explicitly considering the impact of parametric and structural model error. A type of model error not considered in this work is that which results from differences between the model used to perform the linearization and the model used to perform the predictions. This error is often present in NWP situations, and its impact in the adaptive observation context is discussed in Buizza and Montani (1999).

For the model considered in this work, Fig. 8 shows that extremely small analysis uncertainty is required before dynamical information can provide the basis of an AOS that will outperform a solely uncertainty-based AOS. This result, and the AEAOS versus FEAOS result of Fig. 6, conclusively demonstrate the potential benefit of explicitly accounting for the dynamical evolution of uncertainty. The implications of these results to NWP is dependent on the relative magnitude of operational analysis errors; the constraints imposed by the current static observation network, data assimilation schemes and NWP model error will dictate whether an AOS based on model linearizations will be productive.

Acknowledgments. The authors gratefully acknowledge discussions with Kerry Emanuel regarding the results in LE98, and useful comments on the manuscript from Kerry Emanuel and Zoltan Toth. We also wish to thank Mark Berliner and an anonymous reviewer whose efforts greatly improved the manuscript. This work was supported in part by EU Contract ENV4-CT97-0501 and ONR Predictability DRI Grant N00014-99-1-0056.

APPENDIX

Metrics and Singular Vectors

The evolution of uncertainty growth is of extreme interest in the NWP community for the purpose of predictability (Palmer et al. 1994), ensemble construction (Ehrendorfer and Tribbia 1997) and adaptive observations (Lorenz and Emanuel 1998; Palmer et al. 1998; Hansen 1998). Formally, directions of largest uncertainty growth can be determined through the calculation of expected growth factors over a fixed time. Define $\mathbf{f} = [\mathbf{x}^m(t) - \mathbf{x}^a(t)]$ to be the forecast error at $t = t_0 + \tau_{\text{opt}}$, where $\mathbf{x}^m(t)$ is the state of a model integration and $\mathbf{x}^a(t)$ is the system state. Similarly, $\mathbf{g} = [\mathbf{x}^a(t_0) - \mathbf{x}^i(t_0)]$ is the analysis error where $\mathbf{x}^a(t_0)$ is the analyzed state

of the model at t_0 and $\mathbf{x}^i(t_0)$ is the true state of the model at t_0 . Let \mathbf{W}_f be a forecast error weighting matrix that describes the relative importance of forecast errors, and \mathbf{W}_g be an analysis error weighting matrix.

The growth rate of error over τ_{opt} can then be written as

$$\sigma = \frac{\mathbf{f}^T \mathbf{W}_f \mathbf{f}}{\mathbf{g}^T \mathbf{W}_g \mathbf{g}}. \quad (\text{A.1})$$

It is desired to find the directions in state space associated with the growth rates obtained from maximizing σ . Equation (A.1) can immediately be rewritten in the form of a generalized eigenvalue problem, but before doing so, consider the following transformations.

If \mathbf{W}_f and \mathbf{W}_g are symmetric and positive definite, then by Cholesky factorization^{A1}

$$\mathbf{W}_f = \mathbf{P}_f^T \mathbf{P}_f \quad (\text{A.2})$$

$$\mathbf{W}_g = \mathbf{P}_g^T \mathbf{P}_g, \quad (\text{A.3})$$

where \mathbf{P}_f and \mathbf{P}_g are lower triangular matrices. This gives

$$\sigma = \frac{\mathbf{f}^T \mathbf{P}_f^T \mathbf{P}_f \mathbf{f}}{\mathbf{g}^T \mathbf{P}_g^T \mathbf{P}_g \mathbf{g}} \quad (\text{A.4})$$

or, by the change of variables $\mathbf{f}' = \mathbf{P}_f \mathbf{f}$ and $\mathbf{g}' = \mathbf{P}_g \mathbf{g}$

$$\sigma = \frac{\mathbf{f}'^T \mathbf{f}'}{\mathbf{g}'^T \mathbf{g}'}. \quad (\text{A.5})$$

Through linearization of the model equations, the model linear uncertainty propagator, \mathbf{M} , can be constructed so that $\mathbf{f} = \mathbf{M} \mathbf{g}$ or $\mathbf{f}' = \mathbf{P}_f \mathbf{M} \mathbf{g}$. From the change of variables above, \mathbf{g} can be rewritten as $\mathbf{g} = \mathbf{P}_g^{-1} \mathbf{g}'$ giving $\mathbf{f}' = \mathbf{P}_f \mathbf{M} \mathbf{P}_g^{-1} \mathbf{g}'$. This provides a growth factor expression

$$\sigma = \frac{\mathbf{g}'^T \mathbf{P}_f^{-1} \mathbf{M}^T \mathbf{P}_f^T \mathbf{P}_f \mathbf{M} \mathbf{P}_g^{-1} \mathbf{g}'}{\mathbf{g}'^T \mathbf{g}'}, \quad (\text{A.6})$$

which can be expressed as the eigenvalue problem

$$\mathbf{P}_f^{-1} \mathbf{M}^T \mathbf{P}_f^T \mathbf{P}_f \mathbf{M} \mathbf{P}_g^{-1} \mathbf{x} = \lambda \mathbf{x}. \quad (\text{A.7})$$

The maximum growth factors and directions of maximum growth are then given by the eigenvalues and eigenvectors of $\mathbf{P}_f^{-1} \mathbf{M}^T \mathbf{P}_f^T \mathbf{P}_f \mathbf{M} \mathbf{P}_g^{-1}$ or the singular values and singular vectors produced by the SVD of $\mathbf{P}_f \mathbf{M} \mathbf{P}_g^{-1}$.

Consider the weighting matrices of Eq. (A.1). The form of these weightings, or norms, is of great interest in the current predictability literature (Ehrendorfer and Tribbia 1995; Stephenson 1997; Ehrendorfer and Tribbia 1997; Palmer et al. 1998). For predictability studies, the proper initial time norm \mathbf{W}_g is the inverse of the analysis error covariance matrix (Palmer et al. 1998;

^{A1} A special case of LU decomposition for symmetric, positive definite matrices. Cholesky factorization is not the only method for obtaining this type of decomposition. There are a number of other methods for obtaining the "square root" of a matrix (Strang 1988).

Barkmeijer et al. 1998). Applying the inverse of the analysis error covariance matrix as an initial norm results in a set of final time singular vectors that are an estimate of the forecast error covariance matrix. To better understand the impact of an initial time norm, cast Eq. (A.1) as a generalized eigenvalue problem

$$\mathbf{M}^T \mathbf{W}_f \mathbf{M} \mathbf{x} = \lambda \mathbf{W}_g \mathbf{x}. \quad (\text{A.8})$$

For positive definite \mathbf{W}_g and $\mathbf{M}^T \mathbf{W}_f \mathbf{M}$, Eq. (A.8) behaves exactly as a standard eigenvalue problem, but in this case \mathbf{W}_g and $\mathbf{M}^T \mathbf{W}_f \mathbf{M}$ are simultaneously diagonalized. The effect of \mathbf{W}_g is to provide the definition of a hypersphere at initial time (Strang 1988). Neglecting the \mathbf{W}_g (effectively setting it equal to the identity matrix) implies that uncertainties are equally likely in all directions of state space; all analysis error uncertainty information is neglected. Note that *any* choice of \mathbf{W}_g will define an initial time sphere, but the correct choice for most predictability studies is the inverse of the analysis error covariance matrix (Ehrendorfer and Tribbia 1997).

REFERENCES

- Barkmeijer, J., M. VanGijzen, and F. Bouttier, 1998: Singular vectors and estimates of the analysis-error covariance metric. *Quart. J. Roy. Meteor. Soc.*, **124**, 1695–1713.
- Berliner, L. M., Z.-Q. Lu, and C. Snyder, 1999: Statistical design for adaptive weather observations. *J. Atmos. Sci.*, **56**, 2536–2552.
- Bishop, C. H., and Z. Toth, 1999: Ensemble transformation and adaptive observations. *J. Atmos. Sci.*, **56**, 1748–1765.
- Buizza, R., 1995: Optimal perturbation time evolution and sensitivity of ensemble prediction to perturbation amplitude. *Quart. J. Roy. Meteor. Soc.*, **121**, 1705–1738.
- , and T. N. Palmer, 1995: The singular-vector structure of the atmospheric general circulation. *J. Atmos. Sci.*, **52**, 1434–1456.
- , and A. Montani, 1999: Targeting observations using singular vectors. *J. Atmos. Sci.*, **56**, 2965–2985.
- Ehrendorfer, M., and J. J. Tribbia, 1995: Efficient prediction of covariances using singular vectors. Preprints, *Sixth Int. Meeting on Statistical Climatology*, Galway, Ireland, 135–138.
- , and —, 1997: Optimal prediction of forecast error covariances through singular vectors. *J. Atmos. Sci.*, **54**, 286–313.
- Emanuel, K., and Coauthors, 1995: Report of the first prospectus development team of the U.S. weather research-program to NOAA and the NSF. *Bull. Amer. Meteor. Soc.*, **76**, 1194–1208.
- Errico, R. M., T. Vukićević, and K. Raeder, 1993: Examination of the accuracy of a tangent linear-model. *Tellus*, **45A**, 462–477.
- Evensen, G., 1994: Sequential data assimilation with a nonlinear quasi-geostrophic model using Monte Carlo methods to forecast error statistics. *J. Geophys. Res.*, **99**(C5), 10 143–10 162.
- , and P. J. van Leeuwen, 1996: Assimilation of geosat data for the agulhas current using the ensemble kalman filter with a quasi-geostrophic model. *Mon. Wea. Rev.*, **124**, 85–96.
- Gilmour, I., 1998: Nonlinear model evaluation: ν -shadowing, probabilistic prediction and weather forecasting. Ph.D. thesis, Oxford University, 184 pp. [Available from the Bodleian Library, Broad Street, Oxford OX1 3BG, United Kingdom.]
- , and L. A. Smith, 1997: Enlightenment in shadows. *Applied Nonlinear Dynamics and Stochastic Systems Near the Millennium*, J. B. Kadtko and A. Bulsara, Eds., American Institute of Physics, 335–340.
- Hansen, J. A., 1998: Adaptive observations in spatially extended, nonlinear dynamical systems. Ph.D. thesis, Oxford University, 207 pp. [Available from the Bodleian Library, Broad Street, Oxford OX1 3BG, United Kingdom.]
- Joly, A., and Coauthors, 1997: The Fronts and Atlantic Storm-Track Experiment (FASTEX): Scientific objectives and experimental design. *Bull. Amer. Meteor. Soc.*, **78**, 1917–1940.
- , and Coauthors, 1999: Overview of the field phase of the Fronts and Atlantic Storm-Track Experiment (FASTEX) project. *Quart. J. Roy. Meteor. Soc.*, submitted.
- Langland, R., and G. Rohaly, 1996: Adjoint-based targeting of observations for FASTEX cyclones. Preprints, *Seventh Conf. on Mesoscale Process*, Reading, United Kingdom, Amer. Meteor. Soc., 369–371.
- Lorenz, E. N., 1995: Predictability—A problem partly solved. *Proc. ECMWF Seminar on Predictability*, Reading, United Kingdom, ECMWF, 1–18.
- , and K. Emanuel, 1998: Optimal sites for supplementary weather observations: Simulation with a small model. *J. Atmos. Sci.*, **55**, 399–414.
- Palmer, T. N., R. Buizza, F. Molteni, Y. Q. Chen, and S. Corti, 1994: Singular vectors and the predictability of weather and climate. *Philos. Trans. Roy. Soc. London A*, **348**, 459–475.
- , R. Gelaro, J. Barkmeijer, and R. Buizza, 1998: Singular vectors, metrics, and adaptive observations. *J. Atmos. Sci.*, **55**, 633–653.
- Pecora, L. M., and T. L. Carroll, 1990: Synchronization in chaotic systems. *Phys. Rev. Lett.*, **64**, 821–824.
- Smith, L. A., and L. Gilmour, 1998: Accountability and internal consistency in ensemble formation. *Proc. ECMWF Seminar on Predictability*, Reading, United Kingdom, ECMWF, 113–127.
- Stephenson, D. B. 1997: Correlation of spatial climate/weather maps and the advantages of using the Mahalanobis metric in predictions. *Tellus*, **49A**, 513–527.
- Strang, G., 1988: *Linear Algebra and its Applications*. Harcourt Publishers Ltd., 505 pp.
- Toth, Z., and E. Kalnay, 1993: Ensemble forecasting at NMC: The generation of perturbations. *Bull. Amer. Meteor. Soc.*, **74**, 2317–2330.
- Vukićević, T., 1991: Nonlinear and linear evolution of initial forecast errors. *Mon. Wea. Rev.*, **119**, 1602–1611.